SUPPLEMENTAL INFORMATION

BMI1 Inhibition Eliminates Residual Cancer Stem Cells after PD1 Blockade and Activates Antitumor Immunity to Prevent Metastasis and Relapse

Lingfei Jia[1, 2], Wuchang Zhang[1, 2], and Cun-Yu Wang[1, 2, 3, 4*]

Figure S1

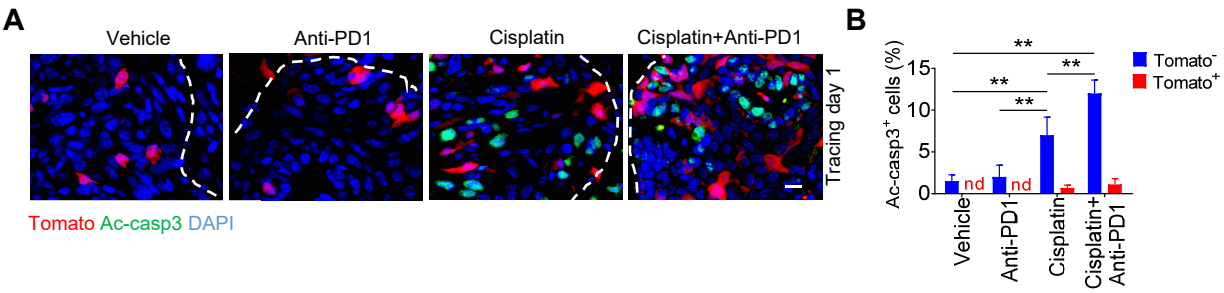

Figure S1, Related to Figure 1, Cisplatin plus anti-PD1 induces apoptosis in HNSCC.

(A) Representative staining for Ac-casp3$^+$ apoptotic cells (green) and Tomato$^+$ CSCs (red) in HNSCC. Nuclei were stained with DAPI (blue). White dashed lines demark tumor-stromal junction. Scale bar, 10 μm.

(B) Quantifications of percentage of Ac-casp3$^+$ cells in Tomato$^+$ and Tomato$^-$ cells in HNSCC. Mean ± SD from the pool of two independent experiments (n = 8). nd, not detected. **p < 0.01 by one-way ANOVA.

Figure S2

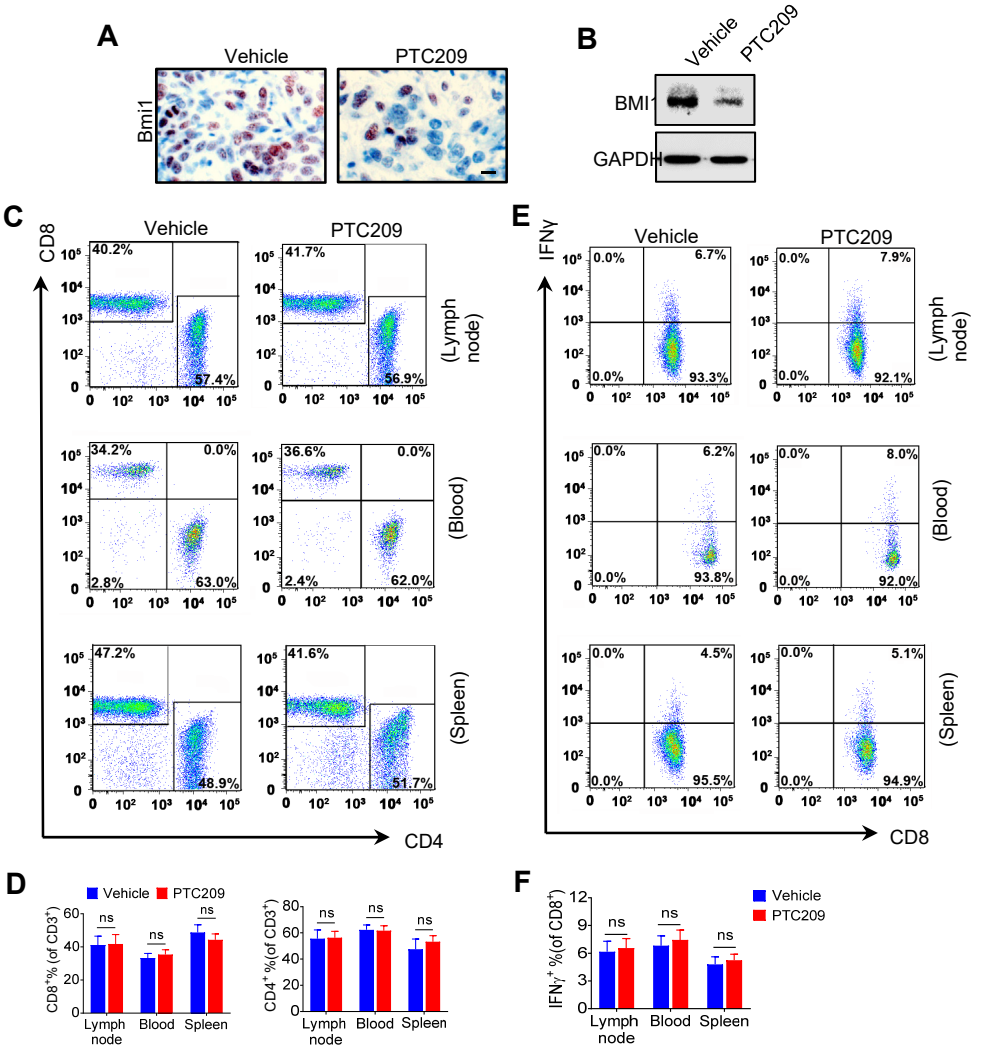

Figure S2, Related to Figure 2, PTC209 treatment does not affect CD8⁺ cell activation in lymph nodes, blood and spleen of mice

(A) Immunochemistry showing the inhibition of BMI1 in HNSCC by PTC209. Scale bar, 10 μm.

(B) Western blot showing the inhibition of BMI1 expression in HNSCC tumor tissues by PTC209 treatment. GAPDH was used as internal control.

(C) Flow cytometry analysis of $CD8^+$ and $CD4^+$ T cells in cervical lymph nodes, blood, and spleen of 4NQO-induced HNSCC mice treated with vehicle and PTC209.

(D) Quantifications of percentage of $CD8^+$ and $CD4^+$ T cells in $CD3^+$ cells in lymph nodes, blood, and spleen of each group as indicated. Values are mean ± SD. n = 6, ns, not significant by unpaired Student's *t* test.

(E) Flow cytometry analysis of percentages of $CD8^+$ T cells expressing IFNγ in cervical lymph nodes, blood, and spleen of 4NQO-induced HNSCC mice treated with vehicle or PTC209.

(F) Quantifications of percentage of $CD8^+$ T cells secreting IFNγ in lymph nodes, blood, and spleen of each group as indicated. Values are mean ± SD, n = 6, ns, not significant by unpaired Student's *t* test.

Figure S3

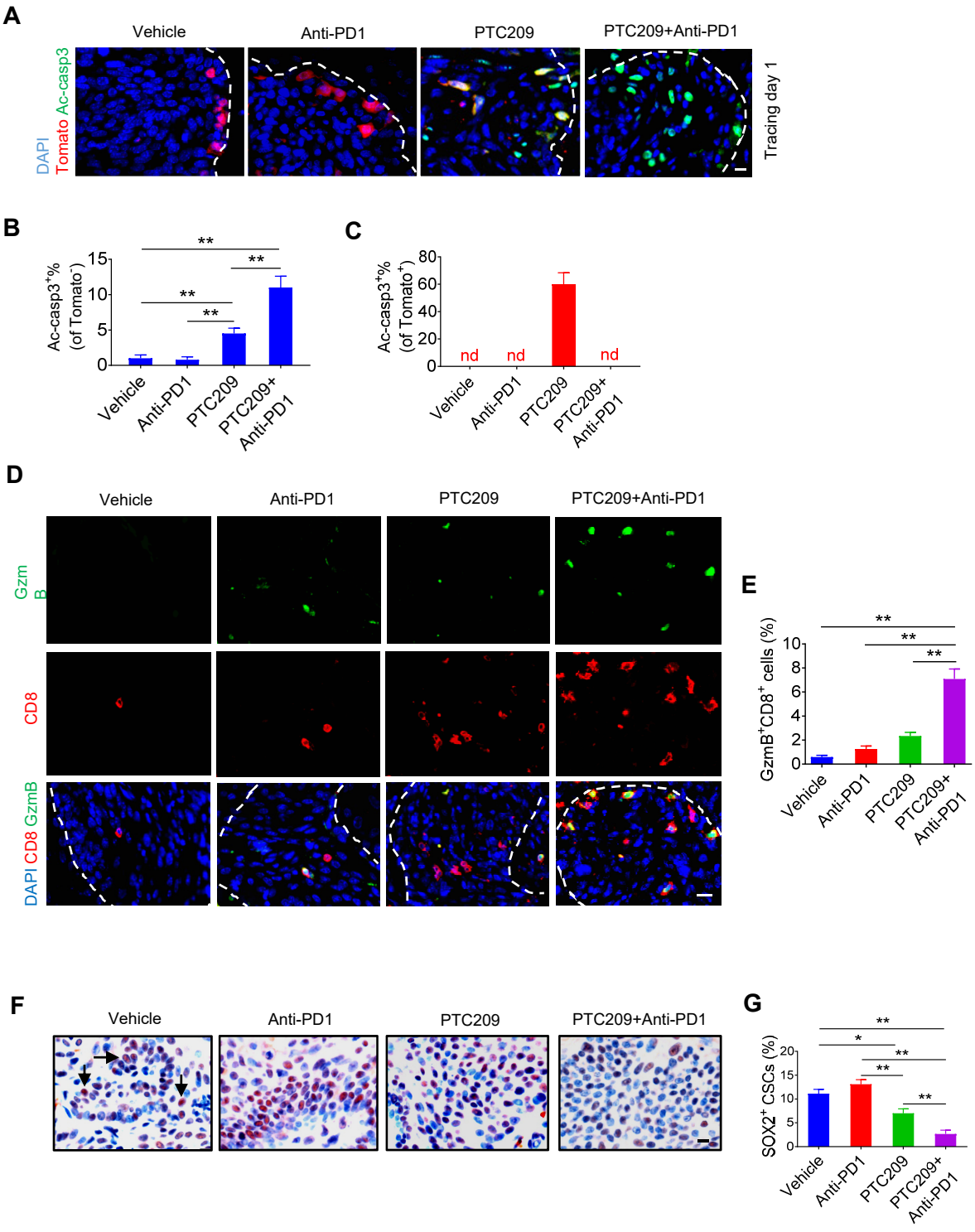
A
Vehicle
Anti-PD1
PTC209
PTC209+Anti-PD1
DAPI
Tomato Ac-casp3
Tracing day 1
B
Ac-casp3+% (of Tomato-)
Vehicle
Anti-PD1
PTC209
PTC209+ Anti-PD1
C
Ac-casp3+% (of Tomato+)
nd
D
Gzm B
CD8
DAPI CD8 GzmB
E
GzmB+CD8+ cells (%)
F
G
SOX2+ CSCs (%)

Figure S3, Related to Figure 2, Anti-PD1 plus PTC209 recruits and activates $CD8^+$ cells in HNSCC.

(A) Representative images of Ac-$casp3^+$ (green) and $Tomato^+$ CSCs (red) in HNSCC. Nuclei were stained with DAPI (blue). White dashed lines demark tumor-stromal junction. Scale bar, 10 μm.

(B) Percentage of Ac-$casp3^+$ cells in $Tomato^-$ cells in HNSCC from mice with treatment as indicated. Values are mean ± SD from the pool of two independent experiments. n = 12, **p < 0.01 by one-way ANOVA.

(C) Quantifications of percentage of Ac-$casp3^+$ in $Tomato^-$ cells in HNSCC. Values are mean ± SD from the pool of two independent experiments. n = 12. nd, not detected.

(D) Representative immunofluorescent images for $CD8^+$ T and $GzmB^+$ T cells. The upper, middle and lower panels respectively show the staining of GzmB (green), CD8 (Red), and CD8 co-localization with GzmB. Nuclei were visualized by DAPI (blue). White dashed lines demark tumor-stromal junction. Scale bar, 10 μm.

(E) Quantifications of percentage of $GzmB^+$ $CD8^+$ T cells percentage in HNSCC. Values are mean ± SD from the pool of two independent experiments. n = 12. **p < 0.01 by one-way ANOVA.

(F) Representative images of $SOX2^+$ cells in HNSCC after treatment. SOX2 staining intensity was scored as: 1 = weak; 2 = moderate; 3 = strong. Only tumor cells with strong SOX2 staining were counted as $SOX2^+$ CSCs. Black arrows indicate $SOX2^+$ CSCs. Scale bar, 10 μm.

(G) Quantification of the percentage of $SOX2^+$ CSCs in HNSCC after treatment. Values are mean ± SD from the pool of two independent experiments. n = 12, *p < 0.05 and **p < 0.01 by one-way ANOVA.

Figure S4

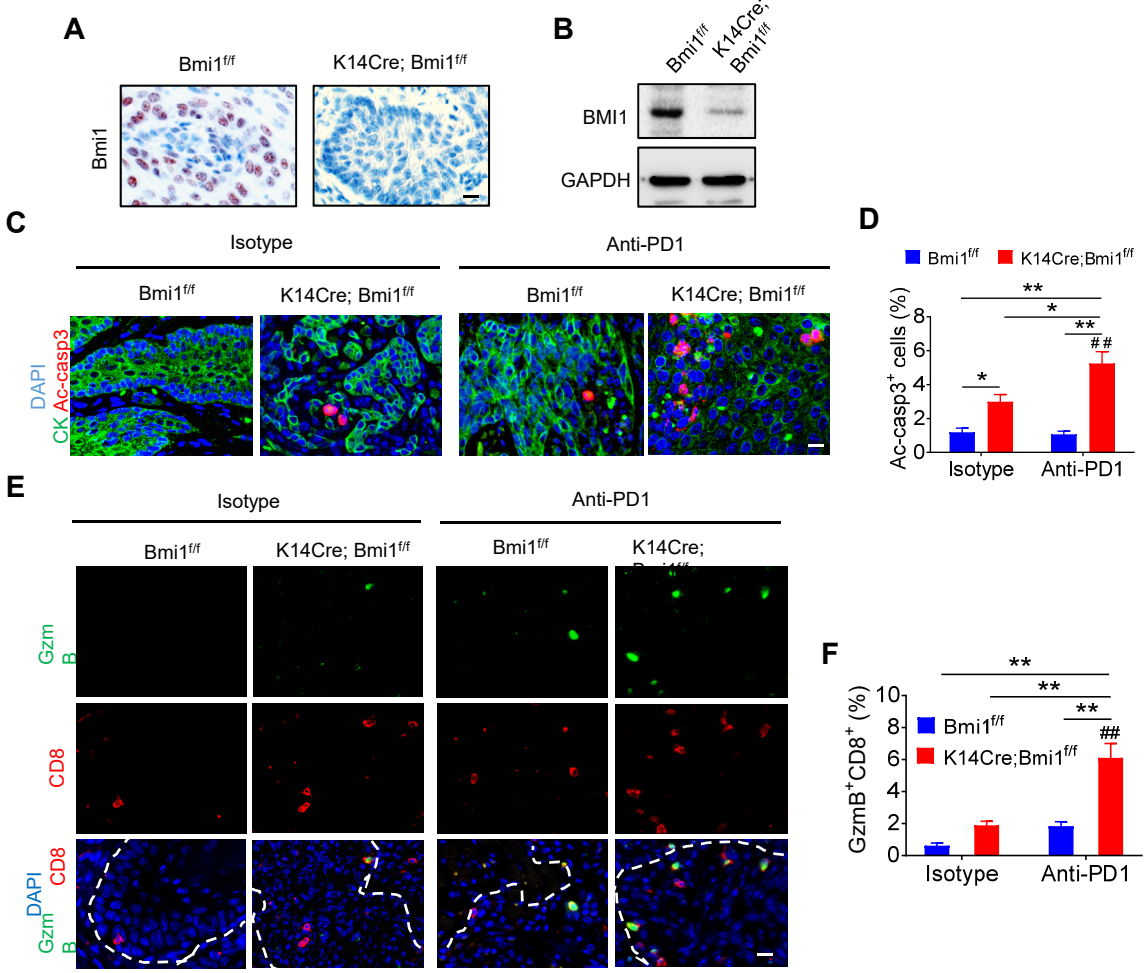

Figure S4, Related to Figure 4, Tumor cell deletion of BMI1 collaborates with anti-PD1 to inhibit HNSCC by recruiting and activating CD8⁺ T cells.

(A) Immunochemical staining of BMI1 in HNSCC from both *Bmi1$^{f/f}$* and *K14Cre;Bmi1$^{f/f}$* mice after Tam treatment. Scale bar, 10 μm.

(B) Western blot showing that BMI1 was deleted in HNSCC from *K14Cre;Bmi1$^{f/f}$*.

(C) Immunostaining of Ac-casp3⁺ apoptotic cells (green) in HNSCC. Nuclei were stained with DAPI (blue). Scale bar, 10 μm.

(D) Percentage of Ac-casp3⁺ cells in HNSCC. Values are mean ± SD from the pool of two independent experiments. n = 14, *p < 0.05 and **p < 0.01 by two-way ANOVA. ##p < 0.01 treatment x genotype interaction.

(E) Immunofluorescent staining of CD8⁺ and GzmB⁺ T cells. The upper, middle and lower panels respectively show the staining of GzmB (green), CD8 (Red), and CD8 co-localization with GzmB. Nuclei were visualized by DAPI (Blue). White dashed lines demark tumor-stromal junction. Scale bar, 10 μm.

(F) Quantifications of percentage of GzmB⁺ CD8⁺ T cells in HNSCC. Values are mean ± SD from the pool of two independent experiments. n = 14, **p < 0.01 by two-way ANOVA. ##p < 0.01 treatment x genotype interaction.

Figure S5

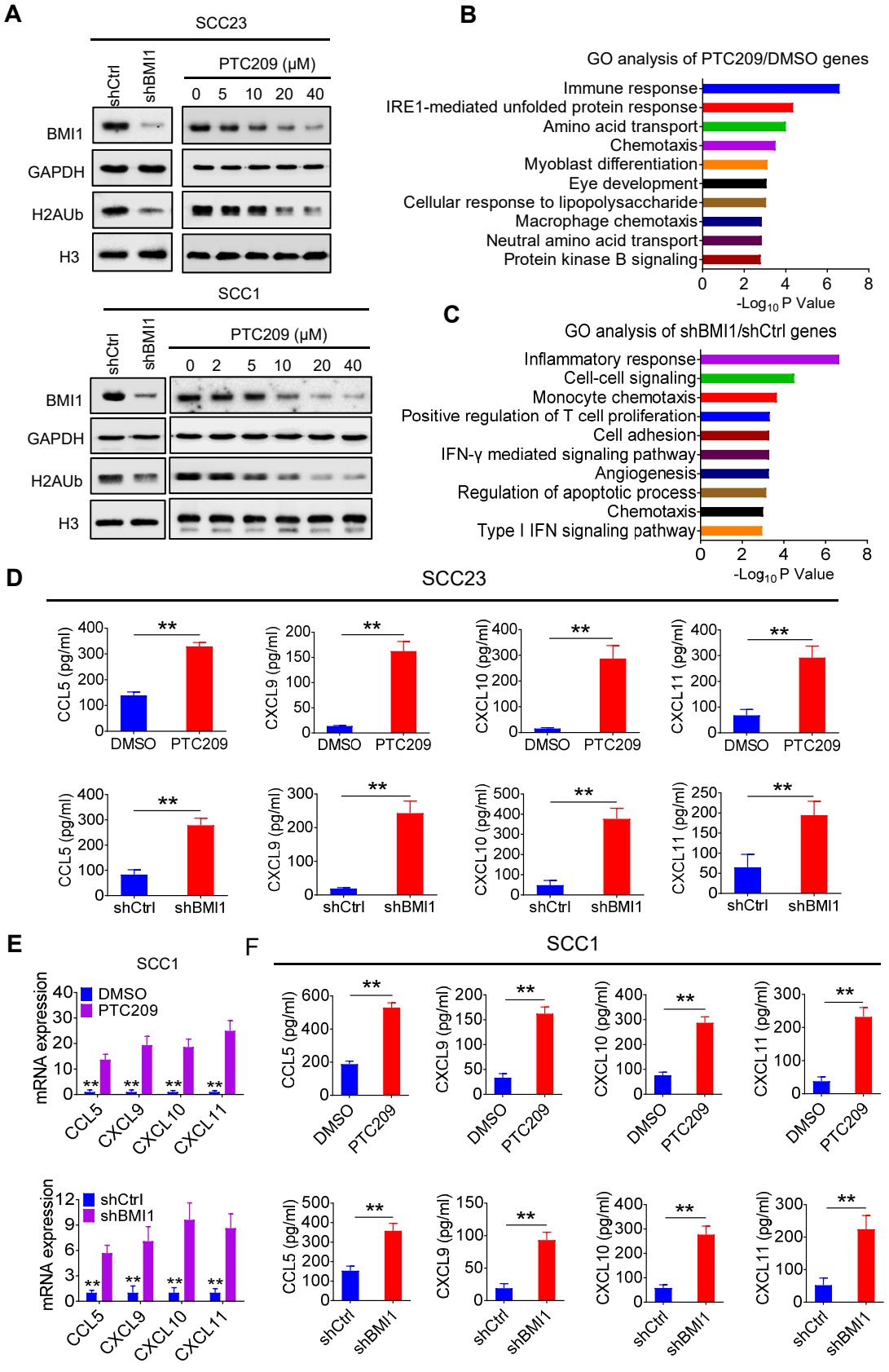
A
SCC23
shCtrl
shBMI1
PTC209 (μM)
0 5 10 20 40
BMI1
GAPDH
H2AUb
H3
SCC1
shCtrl
shBMI1
PTC209 (μM)
0 2 5 10 20 40
BMI1
GAPDH
H2AUb
H3
B
GO analysis of PTC209/DMSO genes
Immune response
IRE1-mediated unfolded protein response
Amino acid transport
Chemotaxis
Myoblast differentiation
Eye development
Cellular response to lipopolysaccharide
Macrophage chemotaxis
Neutral amino acid transport
Protein kinase B signaling
0 2 4 6 8
-Log10 P Value
C
GO analysis of shBMI1/shCtrl genes
Inflammatory response
Cell-cell signaling
Monocyte chemotaxis
Positive regulation of T cell proliferation
Cell adhesion
IFN-γ mediated signaling pathway
Angiogenesis
Regulation of apoptotic process
Chemotaxis
Type I IFN signaling pathway
0 2 4 6 8
-Log10 P Value
D
SCC23
CCL5 (pg/ml)
CXCL9 (pg/ml)
CXCL10 (pg/ml)
CXCL11 (pg/ml)
DMSO PTC209
shCtrl shBMI1
**
E
SCC1
mRNA expression
DMSO
PTC209
shCtrl
shBMI1
CCL5
CXCL9
CXCL10
CXCL11
F
SCC1
CCL5 (pg/ml)
CXCL9 (pg/ml)
CXCL10 (pg/ml)
CXCL11 (pg/ml)
DMSO PTC209
shCtrl shBMI1
**

Figure S5, Related to Figure 5, BMI1 inhibition activates tumor cell-intrinsic anti-tumor immunity in SCC cells.

(A) Western blot analysis of BMI1 and H2Aub in SCC23 and SCC1 treated with shBMI1 or PTC209.

(B) Histogram of the top 10 most-enriched GO terms of upregulated genes (fold change > 2) in SCC23 cells induced by PTC209.

(C) Histogram of the top 10 most-enriched GO terms of upregulated genes (fold change > 2) in SCC23 cells induced by shBMI1.

(D) ELISA showed that the protein levels of CCL5, CXCL9, CXCL10, and CXCL11 in SCC23 cells were induced by PTC209 or *BMI1* knockdown. Means ± SD were shown. **p < 0.01 by unpaired Student's *t* test.

(E) qRT-PCR showed that the expression of CCL5, CXCL9, CXCL10, and CXCL11 in SCC1 cells were induced by PTC209 or *BMI1* knockdown. Means ± SD were shown. **p < 0.01 by unpaired Student's *t* test.

(F) ELISA showed that the protein levels of CCL5, CXCL9, CXCL10, and CXCL11 in SCC1 cells were induced by PTC209 or *BMI1* knockdown. Means ± SD were shown. **p < 0.01 by unpaired Student's *t* test.

Figure S6

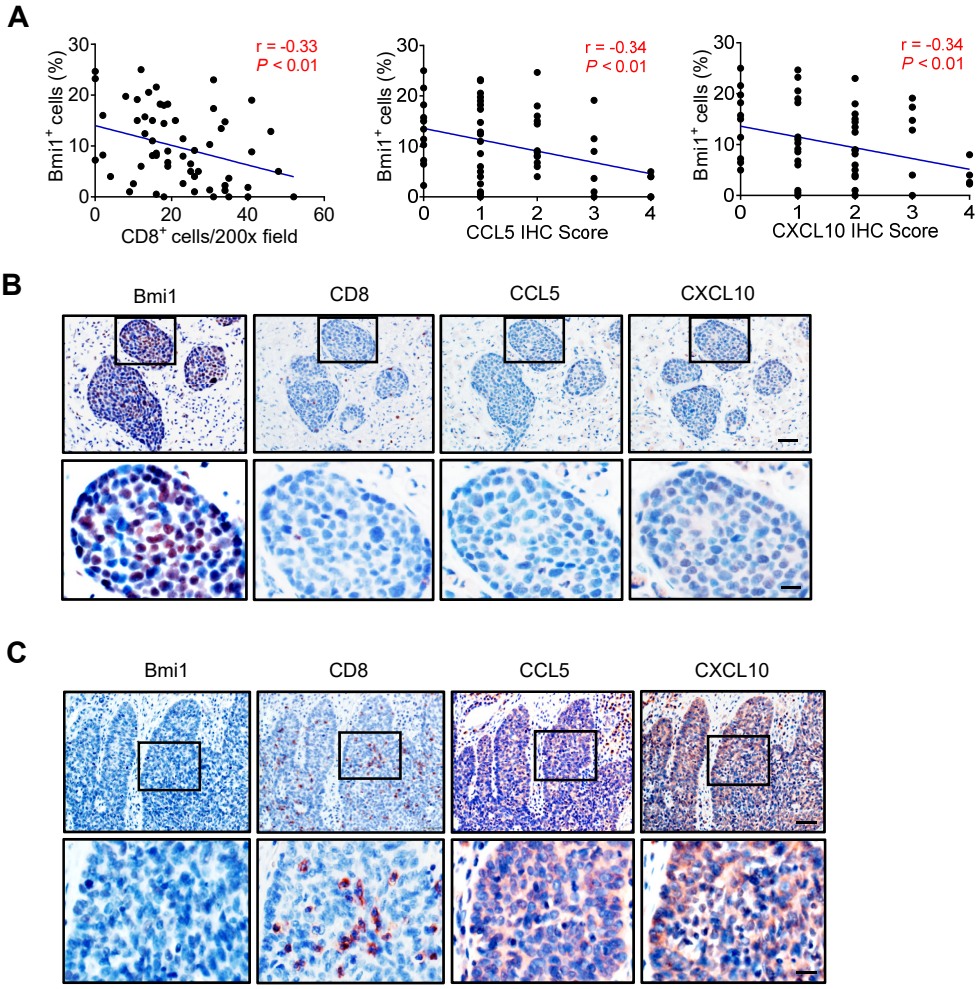

Figure S6, Related to Figure 5, BMI1 protein expression levels are negatively associated with the expression of CD8, CCL5, and CXCL10 in human HNSCC.
(A) BMI1 protein expression levels were negatively correlated with the expression of CD8, CCL5, and CXCL10 in human HNSCC samples (n = 60). The Pearson and Spearman correlation coefficient of liner regression was used to determine the correlation between different proteins.
(B) Representative immunostaining of human HNSCC samples with high BMI1 expression and corresponding low expression of CD8, CCL5, and CXCL10. Scale bar, 200 μm. Enlarged images are shown in the lower panels. Scale bar, 50 μm.
(C) Representative immunostaining of human HNSCC with low BMI1 expression and corresponding high expression of CD8, CCL5, and CXCL10. Scale bar, 200 μm. Enlarged images are shown in the lower panels. Scale bar, 50 μm.

Figure S7

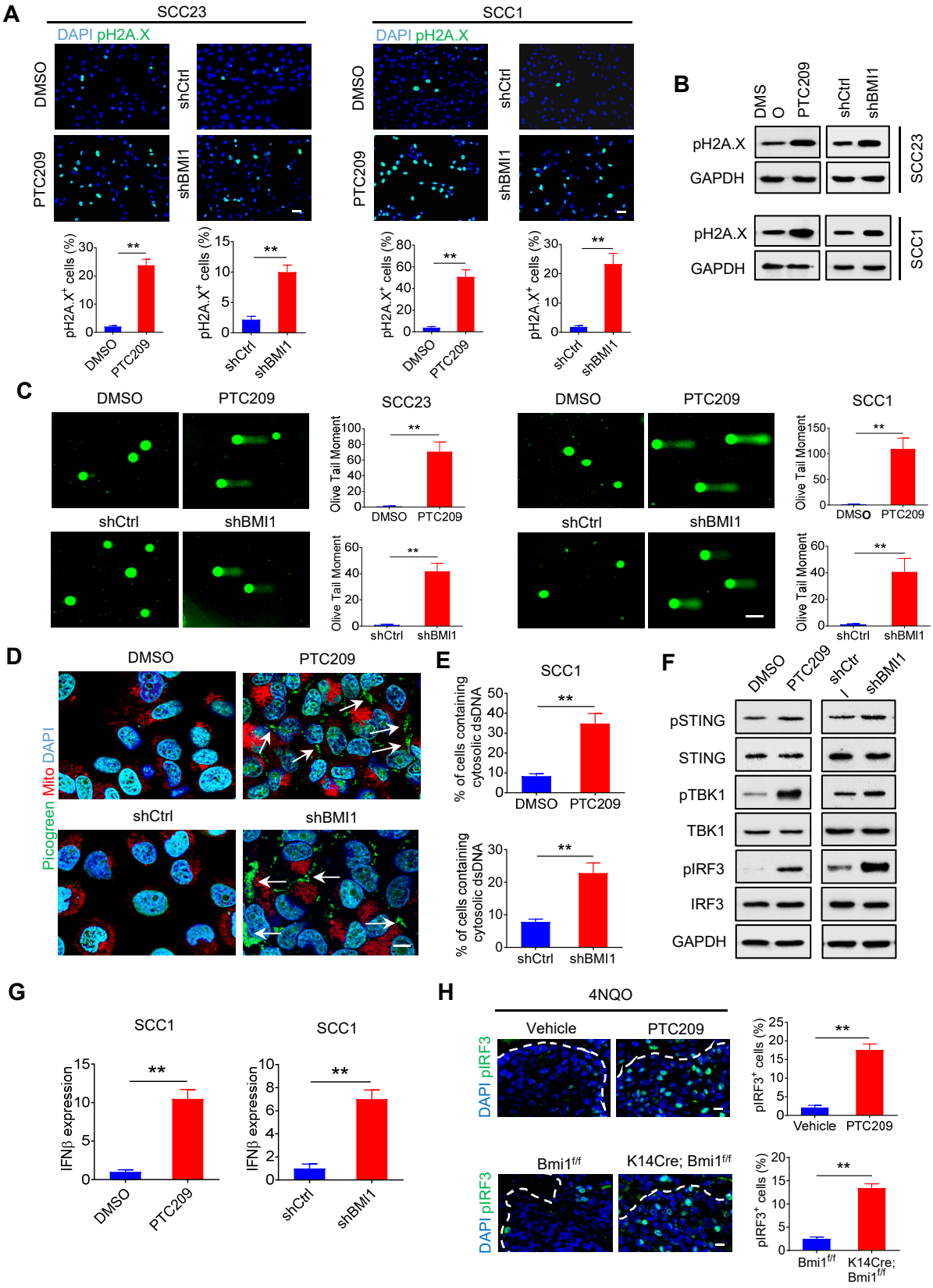
A
SCC23
SCC1
DAPI pH2A.X
DMSO
PTC209
shCtrl
shBMI1
pH2A.X+ cells (%)
B
DMSO
PTC209
shCtrl
shBMI1
pH2A.X
GAPDH
SCC23
SCC1
C
Olive Tail Moment
D
Picogreen Mito DAPI
E
% of cells containing cytosolic dsDNA
F
pSTING
STING
pTBK1
TBK1
pIRF3
IRF3
G
IFNβ expression
H
4NQO
Vehicle
DAPI pIRF3
pIRF3+ cells (%)
Bmi1f/f
K14Cre; Bmi1f/f

Figure S7, Related to Figure 5, BMI1 Inhibition activates cGAS-STING-IRF3 signaling by inducing DNA damage and cytosolic DNA accumulation.

(A) Immunofluorescent staining of pH2A.X (green) in SCC23 and SCC1 cells treated with PTC209 or shBMI1 and their quantifications. Nuclei were stained with DAPI (blue). Means ± SD are from three independent experiments. Scale bar, 50 μm. **p < 0.01 by unpaired Student's *t* test.

(B) Western blot analysis of pH2A.X in SCC23 and SCC1 treated with PTC209 and shBMI1 treatment.

(C) Representative images and quantification of DNA Comet assays in SCC23 and SCC1 cells treated with PTC209 or shBmi1. More than 200 cells were analyzed per group. Means ± SD are shown. Scale bar, 100 μm. **p < 0.01 by unpaired Student's *t* test.

(D) Confocal images showing cytosolic DNA accumulation in SCC1 cells induced by PTC209 or shBMI1. Double strand DNA (dsDNA) were stained by Picogreen (Green). Mitochondria and nuclei were respectively stained with Mito-tracker (Red) and DAPI (Blue). White arrows indicate cytosolic dsDNA. Scale bar, 10 μm.

(E) Quantification of cytosolic dsDNA accumulation in SCC1 cells induced by PTC209 or shBMI1. More than 100 cells were analyzed per group. Means ± SD are shown. **p < 0.01 by unpaired Student's *t* test.

(F) Induction of phosphorylation of STING (S366), TBK1 (S172) and IRF3 (S396) in SCC1 cells by PTC209 or shBMI1 treatment.

(G) qRT-PCR measurement of IFNβ mRNA expression in SCC1 cells treated with PTC209 or shBMI1. Means ± SD are shown. **p < 0.01 by unpaired Student's *t* test.

(H) Immunofluorescent staining of pIRF3 (green) in 4NQO-induced HNSCC by PTC209 or BMI1 knockout and their quantifications. Nuclei were stained with DAPI (blue). Scale bar, 10 μm. Values are means ± SD, n = 8, **p < 0.01 by unpaired Student's *t* test.